Supplemental Data

Connecting the Navigational Clock

to Sun Compass Input

in Monarch Butterfly Brain

Ivo Sauman, Adriana D. Briscoe,
Haisun Zhu, Dingding Shi, Oren Froy,
Julia Stalleicken, Quan Yuan,
Amy Casselman, and Steven M. Reppert

Figure S1. Arthropod Opsin Phylogeny

The phylogeny is based on a neighbor-joining analysis of 1st + 2nd nucleotide positions, using the Tamura-Nei model with a correction for heterogeneous patterns of evolution among lineages. The majority of full-length opsin sequences included in this tree are homologs of opsins expressed in the insect rhabdomeric photoreceptor cells. Numbers indicate bootstrap replicates out of 500 in which a particular node is supported. Red indicates cloned monarch opsin cDNAs. GenBank accession numbers for the sequences used in the reconstruction are as follows: CHELICERATES, *Limulus polyphemus* (lateral eye, L03781; ocelli, L03782); CRUSTACEANS, *Procambarus clarkii* (S53494); INSECTS, *Anopheles gambiae* (GPRop1-9, accession numbers are given as supplementary information in [Hill et al., 2002]); *Antheraea pernyi* (AB073299); *Apis mellifera* (UV, AF004169; Blue, AF004168; LW, U26026); *Bombyx mori* (Boceropsin, AB064496); *Camponotus abdominalis* (LW, U32502; SW, AF042788); *Cataglyphis bombycinus* (LW, U32501; SW, AF042787); *Drosophila melanogaster* (Rh1, K02315; Rh2, M12896; Rh3, M17718; Rh4, M17730; Rh5, U67905; Rh6, Z86118); *Manduca sexta* (Manop1, L78080; Manop2, L78081; Manop 3, AD001674); *Megoura viciae* (UV, AF189715; LW, AF189714); *Papilio glaucus* (PglRh1, AF077189; PglRh2, AF077190; PglRh3, AF067080; PglRh4, AF077193; PglRh5, AF077191; PglRh6, AF077192); *Pieris rapae*; (PrL, AB177984; Piceropsin, AB086066); *Schistocerca gregaria* (Lo1, X80071; Lo2, X80072); *Sphodromantis* sp. (X71665); *Vanessa cardui* (LW, AF385333).

Note: Full-length nucleotide sequences for the *Bombyx mori* UV, blue, and LW opsin coding regions were obtained using a tBlastx search of GenBank whole-genome sequences (wgs), manually removing the introns in MacClade, and then comparing the coding sequences with partial *B. mori* opsin cDNAs reported in Shimizu et al. (1998). Bar corresponds to the number of substitutions/site.

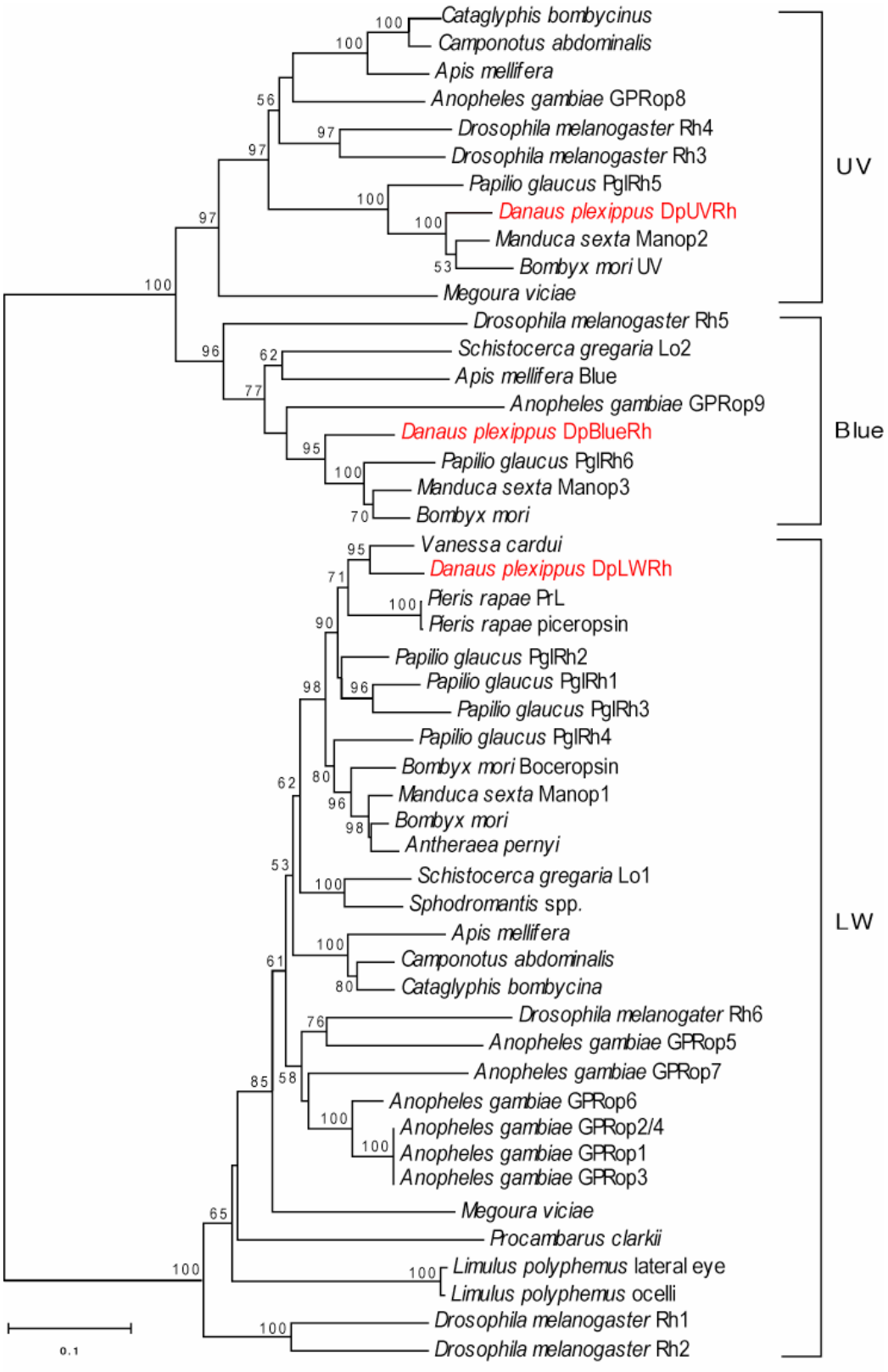
Cataglyphis bombycinus
Camponotus abdominalis
Apis mellifera
Anopheles gambiae GPRop8
Drosophila melanogaster Rh4
Drosophila melanogaster Rh3
Papilio glaucus PglRh5
Danaus plexippus DpUVRh
Manduca sexta Manop2
Bombyx mori UV
Megoura viciae
Drosophila melanogaster Rh5
Schistocerca gregaria Lo2
Apis mellifera Blue
Anopheles gambiae GPRop9
Danaus plexippus DpBlueRh
Papilio glaucus PglRh6
Manduca sexta Manop3
Bombyx mori
Vanessa cardui
Danaus plexippus DpLWRh
Pieris rapae PrL
Pieris rapae piceropsin
Papilio glaucus PglRh2
Papilio glaucus PglRh1
Papilio glaucus PglRh3
Papilio glaucus PglRh4
Bombyx mori Boceropsin
Manduca sexta Manop1
Bombyx mori
Antheraea pernyi
Schistocerca gregaria Lo1
Sphodromantis spp.
Apis mellifera
Camponotus abdominalis
Cataglyphis bombycina
Drosophila melanogater Rh6
Anopheles gambiae GPRop5
Anopheles gambiae GPRop7
Anopheles gambiae GPRop6
Anopheles gambiae GPRop2/4
Anopheles gambiae GPRop1
Anopheles gambiae GPRop3
Megoura viciae
Procambarus clarkii
Limulus polyphemus lateral eye
Limulus polyphemus ocelli
Drosophila melanogaster Rh1
Drosophila melanogaster Rh2
0.1
UV
Blue
LW

Figure S2. Localization of *DpUVRh* and *DpBlueRh* mRNA Transcripts in Main Retina
(A) Montage of a lateral semitangential section, showing that the *DpUVRh* transcript is uniformly expressed across the eye in a majority of ommatidia.
(B) Montage of a section adjacent to (A), showing that *DpBlueRh* transcript is also uniformly distributed across the eye and is expressed in more ommatidia than is *DpUVRh*. The differences in *DpUVRh* and *DpBlueRh* riboprobe localization and intensity between the semitangential adjacent sections seem to be due to slight variations in photoreceptor morphology (unpublished observations) where the photoreceptor cells that express the DpUVRh opsin mRNA appear to be widest distally, and those that express the DpBlueRh opsin mRNA are more variable in morphology where they appear to become widest. This is particularly evident in in situ hybridization performed on dissociated ommatidia where it is easiest to visualize the pattern of opsin mRNA expression across the entire length of the ommatidium (data not shown). Arrow indicates the direction of the antenna base.

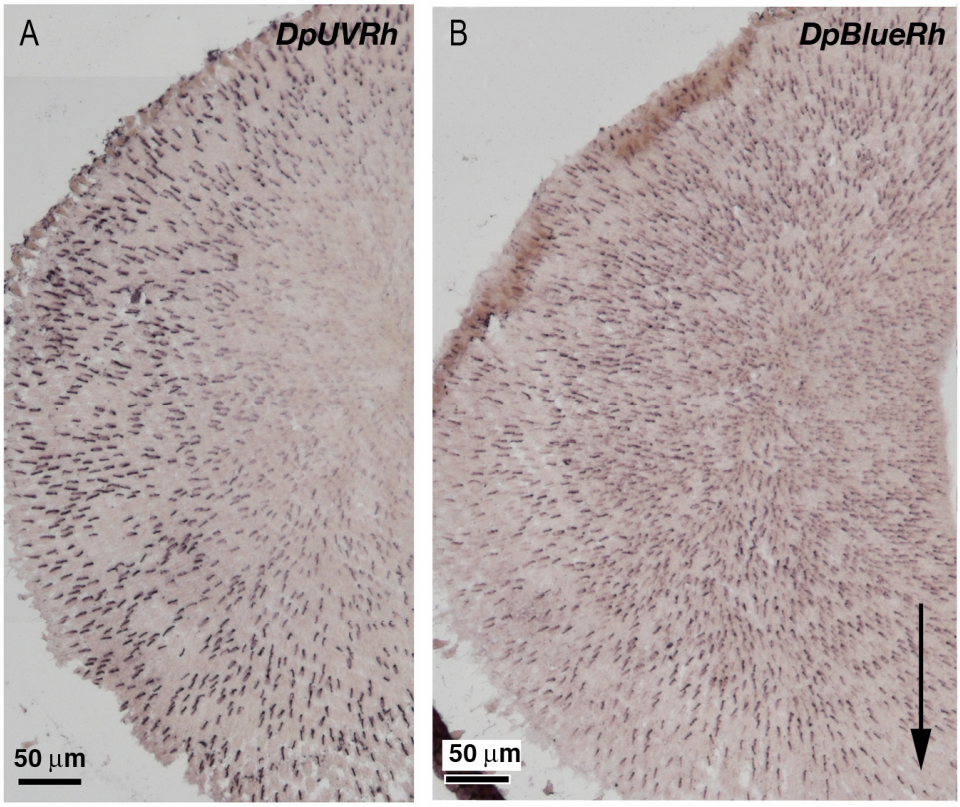

Figure S3. The Effect of UV Interference on Flight Orientation
Sequential records of flight orientation are shown as circular histograms, with each column showing data for a different butterfly (A–C). Flight records in the presence of a UV-interference filter are colored red. The UV-interference filter was removed between the second and third flight records shown in each column. Each circular histogram is a flight record of 5–7 min with sampling at 200 ms intervals. The only exception was the middle record for (A), which was recorded for only 2.7 min, after which the butterfly stopped flying. For each circular histogram, a calculated virtual flight path is depicted in the square to the right. 0° is North. The upper record of (A) is replotted from the lower record of Figure 1A, as the effect of UV interference alone was examined after rotation of the polarizing filter with UV interference. The lower records of (B) and (C) are replotted from the upper panels of Figures 1B and 1C, respectively, as the effect of UV interference alone was examined first for these butterflies.

The butterfly in (A) circled continually for 2.7 min and then stopped flying when the UV-interference filter was placed. Flight was immediately reinitiated when the UV-interference filter was removed (lower panel). This individual continued to orient in the same general direction as before UV interference (299° before versus 295° after).

The butterfly in (B) continued to orient directionally, although flight direction changed from 268° before UV interference to 305° during UV interference. During the recovery period, this individual continued flight orientation in the same general direction (293°). The continued directional flight of the butterfly in (B), in the face of UV interference, could reflect continued inertia to fly in the same direction without polarizing light cues, as for the butterfly in Figure 1D (third record down).

The butterfly in (C) exhibited directional orientation that was severely blunted by UV interference, as the butterfly manifested circling behavior (see Figure 2C, red record). During the recovery period (bottom panel), this individual returned to a bimodal pattern of orientation, but with a shift of the major direction of orientation from 312° before UV interference to 165° during the recovery interval (Figure 2C, upper and lower panels).

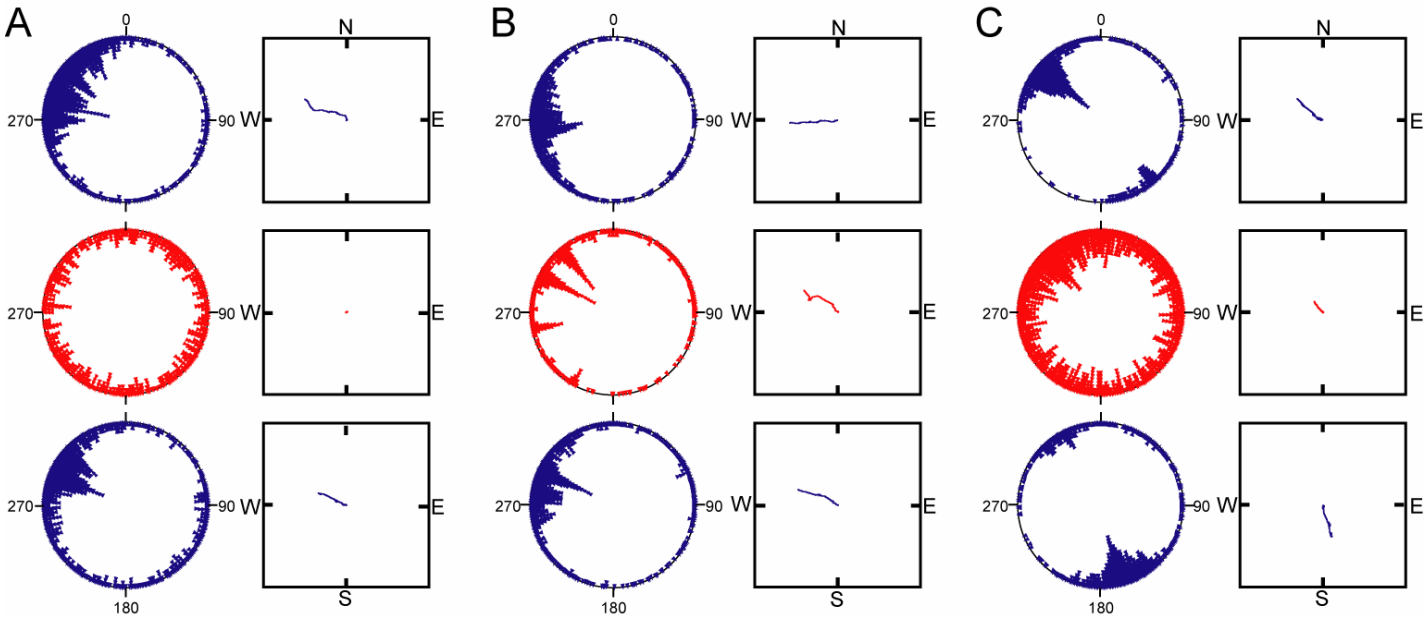

Figure S4. **TIM-Like Immunoreactivity in Adult Monarch Cephalic Nervous System**
(A) Schematic diagram illustrating the topography of TIM-immunoreactive cells.
(B) TIM-like immunoreactivity in pars intercerebralis (PI).
(C) TIM-like immunoreactivity in pars lateralis (PL).

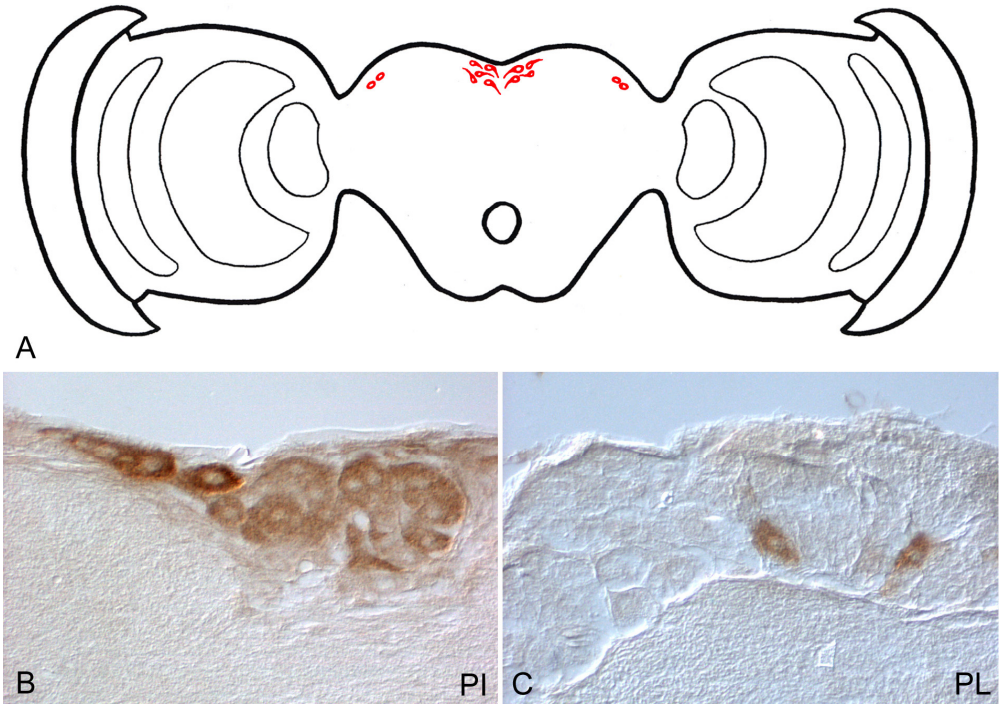

Figure S5. **Phylogenetic Tree of Members of the Photolyase/Cryptochrome Family**
Bootstrap values (of 1000 replicates) are indicated on horizontal branches. The CLUSTAL X program was used to analyze the following amino acid sequences (GenBank™ accession number). Insect Cryptochromes (as marked): *D. plexippus*, dpCRY (AY860425); *A. gambiae*, agCRY (ENSANGP00000013343); *A. pernyi*, apCRY (AAK11644); *D. melanogaster*, dCRY (AAC83828). Vertebrate Cryptochromes: *Mus musculus*, mCRY1 (NP_031797), mCRY2 (AAD46561); *Homo sapiens*, hCRY1 (NP_004066), hCRY2 (NP_066940); Chicken (*Gallus gallus*), gCRY1 (NP_989576), gCRY2 (NP_989575); *Xenopus laevis*, xCRY1 (AAK94665), xCRY2a (AAK94666), xCRY2b (AAK94667); zebrafish (*Danio rerio*), zCRY1a (BAA96846), zCRY1b (BAA96847), zCRY2a (BAA96848), zCRY2b (BAA96849), zCRY3 (BAA96850), zCRY4 (BAA96851). Plant Cryptochromes: *Arabidopsis thaliana*, atCRY1 (Q43125), atCRY2 (Q96524); Tomato (*Lycopersicon esculentum*), leCRY1 (AAF72555), leCRY2 (AAF72556); Pea (*Pisum sativum*), psCRY1 (AAS79662), psCRY2a (AAS79665), psCRY2b (AAS79667); Horseradish (*Armoracia rusticana*), arCRY2 (BAC67179). Photolyases: *D. melanogaster*, dPHR6-4 (BAA12067); *A. gambiae*, agPHR6-4 (ENSANGP00000013343); zebrafish (*Danio rerio*), zPHR6-4 (BAA96852); *X. laevis*, xPHR6-4 (BAA97126); *Monodelphis domestica*, mdPHR (S50083); *A. thaliana*, atCPD (CAA67683); *Halobacterium salinarum*, hsPHR1 (NP_280501), hsPHR2 (NP_280191); *Gloeobacter violaceus*, gvPHR (NP_923781); *Escherichia coli*, ecPHR (P00914). ecPHR was used as the outgroup.

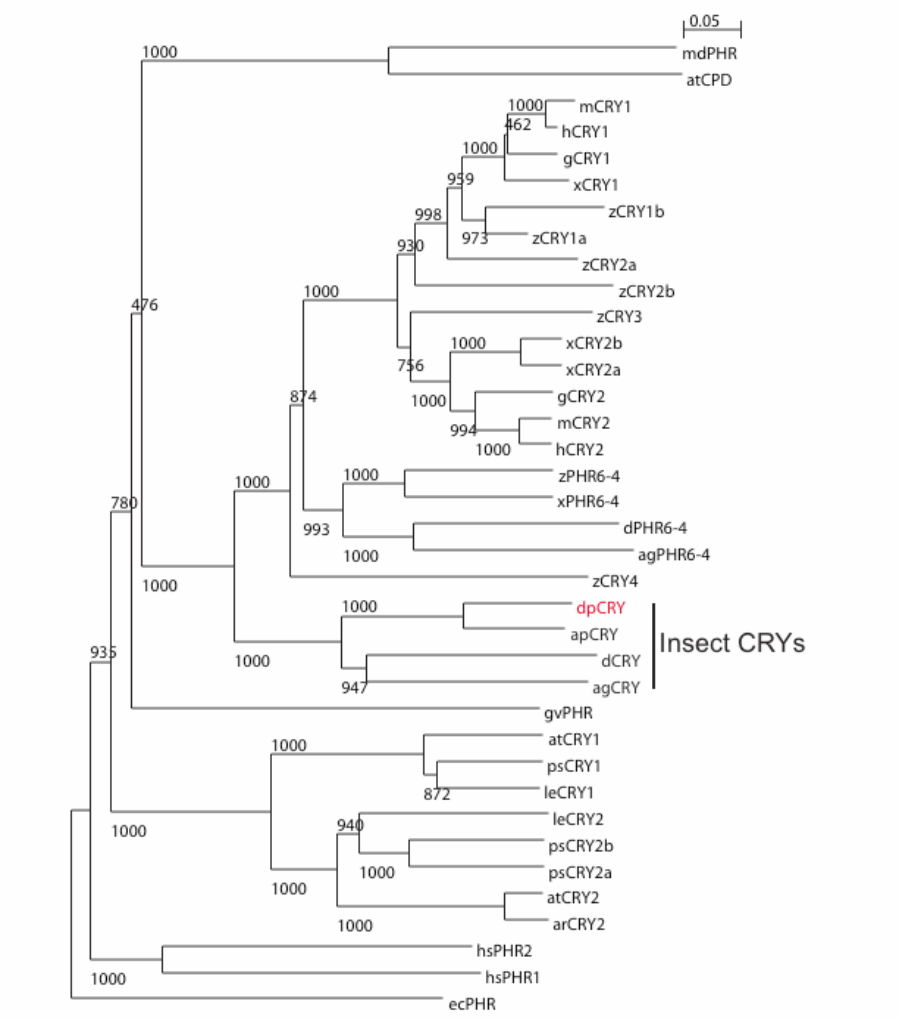

.

Figure S6. **Specificity of Anti-dpCRY Antibodies**
(Upper panel) Western blot of V5-tagged dCRY, apCRY, and dpCRY expressed in S2 cells and probed with anti-dpCRY-1-GP; similar results were found when dpCRY-1-R was used.
(Lower panel) Western blot of the three insect CRYs expressed in S2 cells as in the blot above but probed with the anti-V5-antibody.

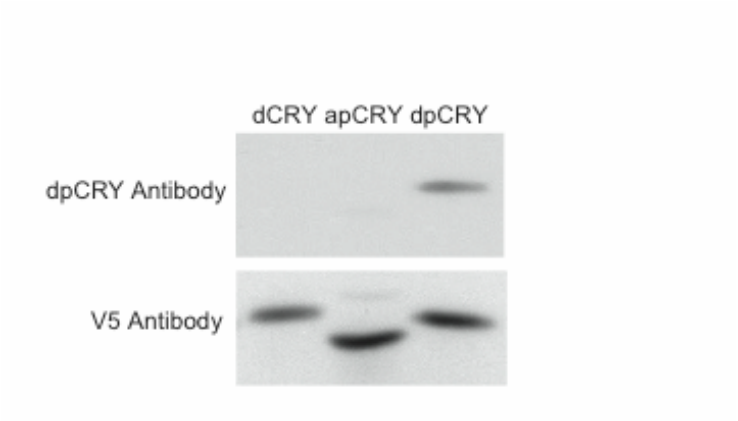

Supplemental Reference

Shimizu, I., Yamakawa, Y., Minamoto, T., and Sakamoto, K. (1998). Cloning of genes encoding the visual pigments in the silkworm, Bombyx mori. Appl. Entomol. Zool. (Jpn.) *33*, 199–204.